Contact Time in Random Walk and Random Waypoint: Dichotomy in Tail Distribution*

Chen Zhao and Mihail L. Sichitiu

Department of Electrical and Computer Engineering,
North Carolina State University, Raleigh, NC 27606, USA
{czhao4,mlsichit}@ncsu.edu

Abstract. Contact time (or link duration) is a fundamental factor that affects performance in Mobile Ad Hoc Networks. Previous research on theoretical analysis of contact time distribution for random walk models (RW) assume that the contact events can be modeled as either consecutive random walks or direct traversals, which are two extreme cases of random walk, thus with two different conclusions. In this paper we conduct a comprehensive research on this topic in the hope of bridging the gap between the two extremes. The conclusions from the two extreme cases will result in a power-law or exponential tail in the contact time distribution, respectively. However, we show that the actual distribution will vary between the two extremes: a power-law-sub-exponential dichotomy, whose transition point depends on the average flight duration. Through simulation results we show that such conclusion also applies to random waypoint.

Keywords: mobile ad hoc network, random walk, random waypoint, contact time, dichotomy.

1 Introduction

Due to the lack of real deployments of Mobile Ad-Hoc Networks (MANETs), current research on this topic is still largely based on simulation. Therefore the behavior of mobility models greatly affects simulation performance [1]. Among numerous mobility models, Random Walk (RW) and Random Waypoint (RWP) are the most widely used ones [2, 3] due to their simplicity, even though many researchers have pointed out that they have many drawbacks [4, 5, 6], and proposed several new ones [7, 8, 9, 10, 5]. However, even for the simple models like RW and RWP, the relationship between their input parameters (speed, pause, flight length, flight directions, etc.) and the corresponding impact on network performance is not yet quantitatively understood.

For dense MANETs with dynamic routing protocols, network performance depends on both the mobility and the protocols. In [1] the authors proposed several protocol independent metrics including the link change rate and link

* This research was supported by NSF grant NSF-0626850.

J. Zheng et al. (Eds.): ADHOCNETS 2009, LNICST 28, pp. 333–348, 2010.

duration, allowing the impact of mobility models to be evaluated through those metrics without reference to any specific protocol. For MANETs with sparser nodes, e.g., Pocket Switched Networks (PSN) [11], there are also such protocol independent metrics like the inter-contact time and the contact time [12].

In both scenarios the contact time (or alternatively, link duration, link lifetime, link expiration time, etc.[1]) has been an important performance metric in evaluating the impact of mobility. In this paper we focus on the distribution of contact times of RW and RWP. Several papers studying this distribution have been published [13, 14, 15, 16, 17, 18, 19, 20, 21]. Some of them are based on empirical analysis [15,19], while others are based on theoretical derivation [13,14,16,17,18,20,21].

Studies based on empirical analysis have the advantage of being accurate. In [15] the authors examined the PDFs of contact time through simulation and concluded that the PDFs are significantly different among different models. Among them the PDF of RW exhibits a single peak. The authors of [19] fit the PDF of contact time from RWP traces against several common distributions. The results showed that the lognormal distribution is the best fit for their traces.

Since it is very hard for the empirical analysis to go through all parameter spaces, theoretical derivation is necessary to better understand the underlying dynamics between the model parameters and the contact time, even though such derivation usually imposes simplifying assumptions. In RW and RWP, nodal movements are consecutive flights along straight lines. When the communication range is small in comparison to the flight length, it is reasonable to assume nodes do not stop or change directions during contact events. Thus the contact events are modeled as *direct traversals* [14,16,17,18]. In an early work [14] using this model, the duration distribution of two-hop paths with static sender and receiver was studied. In [16], the authors derived the contact time distribution of RW using the direct traversal model, assuming all nodes move at the same speed. In their later work [17] they extended the results with heterogeneous nodal speed. Both papers did not derive any closed form and all results were obtained numerically. In [18], the authors did a similar analysis as in [16] but derived a closed form for homogeneous speeds. They also obtained the contact time distribution numerically for two nodes with different fixed speeds.

On the other hand, when the communication range is large in comparison to the flight length, nodes often stop or change directions multiple times during contact events. Thus the contact events should then be modeled as the sum of *consecutive random walks* inside the nodes' communication range (usually modeled as circles) [13,20,21]. In an early work [13] using this model, the authors derived the probability of link availability with different initial conditions. In [20] the authors proposed a two-state Markovian framework that can be used to approximate the contact time distribution of any mobility model. They also stated that the "direct traversal" model is a special case in their framework. A comprehensive analysis of contact times using this model was done in [21], where the authors concluded that the contact time distribution can be approximated

[1] All these terms refer to the same metric. In this paper the term contact time is used.

as exponential. In [21] the communication range is a random variable and the mobility model was a "smoothed" variation of RW [9]. As a special case, their conclusion also applies to ordinary RW with constant communication range.

However, both assumptions, direct traversal and consecutive random walk, are essentially two extremes in regarding the ratio of communication range and flight length. In general, the actual behavior of RW models lies in between the two extremes. In this paper we conduct a comprehensive analysis that bridge these two extreme assumptions in previous works. Especially, we investigate their difference in tail behavior. We first show that when flight lengths are infinite, which is equivalent to the direct traversal assumption, the PDF of contact time has a power law tail with both homogeneous and uniform speed distribution. Moreover, when flight lengths are no longer infinite, the contact time distribution shows a *power-law-sub-exponential dichotomy*, with the transition point being a function of the flight time distribution. As the average flight length becomes shorter, the transition takes place earlier. When, finally, the flight length is short enough in comparison to the communication range, which is equivalent to the consecutive random walk assumption, the dichotomy degenerates into a single exponential tail, which conforms to the conclusion in [21].

The rest of the paper is organized as follows: in Section 2 the main theoretical analysis is performed. The results are validated in Section 3. Section 4 concludes the paper.

2 Model Analysis

In this section the mathematical analysis of the contact time distribution is presented. In Section 2.1 we present the basic settings and assumptions. In Section 2.2 we briefly review the general derivation of contact time distribution in [16, 17, 18] assuming infinite flight lengths. In Section 2.3 the power-law tail behavior is investigated assuming both homogeneous and uniform speed distribution. In Section 2.4 we consider the impact of finite flight length and reach the conclusion of the power-law-sub-exponential dichotomy.

2.1 Model Settings and Assumptions

Random Walk. In the RW model all nodes randomly walk along straight line segments. These walks are called "flights". For each flight a node travels in a direction ϕ at speed v for distance u. Afterwards it pauses for time t_{p}, and starts the next flight.

Parameters ϕ, v, u and t_{p} are independent random variables for each flight. Flights of different nodes are also independent of each other. Usually, the direction ϕ is uniformly distributed over $[0, 2\pi]$, and the speed v is uniformly distributed over $[v_{\min}, v_{\max}]$ ($v_{\min} > 0$ as to obtain a stationary speed distribution [4]). The flight length u and pause time t_{p} usually follow some common distributions like uniform, exponential or even power-law [5] [22].

Throughout this paper, all these assumptions are applied for RW models, except the pause time t_{p} is always ignored (fixed to zero). In addition, nodes are confined to a torus, which provides uniform node density and edge wrapping.

Random Waypoint. RWP differs from RW in that for each flight every node selects a waypoint in a confined area as the destination instead of selecting the direction and the distance. Thus in RWP the node density is not uniform [23], the flight directions may not be uniformly distributed, and the flight length distribution is determined by the shape of the confined area [24]. Directions and distances of consecutive flights of the same node are not independent either. Therefore RWP is far more difficult to analyze than RW.

All analysis in this paper is based on RW models, but the conclusions will also be validated against RWP through simulation in Section 3. The results show that the conclusions obtained from RW hold sufficiently well for RWP.

Contact Event. Every node is assumed to have the same communication range r, which is reasonable under most circumstances. When the distance between two arbitrary nodes N_i and N_j is smaller than r, the two nodes are considered to be able to communicate with each other, and vice versa. If during the time interval $[t_0, t_1]$ the nodes N_i and N_j are able to communicate, while at the time instants t_0^- and t_1^+ they are not, then the time interval $[t_0, t_1]$ is referred to as a *contact event*, and its duration $t_1 - t_0$ is defined as the *contact time*.

2.2 Random Walk with Infinite Flight Lengths

We start with the assumption that all flights have infinite flight lengths so that the contact events are modeled as direct traversals as in [16, 17, 18]. More accurately, this is the limit case as the nodal flight lengths approach infinity.[2] Figure 1 shows such a contact event. Nodes N_i and N_j are moving at velocity $\boldsymbol{v}_i$ and $\boldsymbol{v}_j$, respectively. From N_j's point of view, N_i is moving at the relative velocity:

$$\boldsymbol{v}_{ij} = \boldsymbol{v}_i - \boldsymbol{v}_j. \tag{1}$$

The duration of N_i traversing N_j's contact region (the dashed circle in Fig. 1) is:

$$t_{\mathrm{I}} = \frac{s}{v_{\mathrm{r}}} = \frac{s}{v_{ij}}, \tag{2}$$

where s is the length of the chord, and v_{r} is the traversing speed *during a contact event* which equals to the relative speed v_{ij} (but with different distributions [16, 17, 18]), and t_{I} is the contact time assuming infinite flight lengths.

[2] There is subtle difference between infinite and "approaching infinite" flight lengths. With strict infinite flight lengths, nodes never change their speeds so (8) does not hold. Since we are more interested in finding the limit when flight lengths approach infinity, we obtain the results here and in Section 2.3 assuming (8) holds.

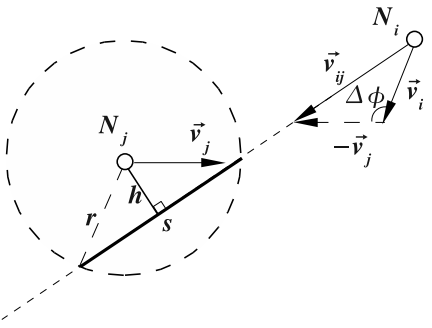

Fig. 1. N_i and N_j are moving at velocity $\boldsymbol{v}_i$ and $\boldsymbol{v}_j$. Both with communication range r. From N_j's perspective, N_i is traversing N_j's contact region (the dashed circle) at the relative velocity $\boldsymbol{v}_{ij}$ along the thick chord s.

Derivation of the distribution of t_I requires the distribution of both s and v_r. Its general derivation is already done in [16, 17, 18]. Due to page limit we just show the results here (with slightly different notation that conforms to ours):

The PDF of the traversal duration t_I assuming infinite flight lengths:

$$f_{T_\mathrm{I}}(t_\mathrm{I}) = \int_0^{2v_\mathrm{max}} f_{V_\mathrm{r}}(v_\mathrm{r}) f_S(v_\mathrm{r} t_\mathrm{I}) v_\mathrm{r} \mathrm{d}v_\mathrm{r}, \tag{3}$$

where f_S is the PDF of the chord length s:

$$f_S(s) = \frac{s}{2r\sqrt{4r^2 - s^2}}, \tag{4}$$

and f_{V_r} is the PDF of the traversal speed v_r:

$$f_{V_\mathrm{r}}(v_\mathrm{r}) = \frac{v_\mathrm{r} f_{V_{ij}}(v_\mathrm{r})}{\int_0^{2v_\mathrm{max}} v_{ij} f_{V_{ij}}(v_{ij}) \mathrm{d}v_{ij}}, \tag{5}$$

where $f_{V_{ij}}$ is the PDF of the relative speed v_{ij} in (1) and (2):

$$f_{V_{ij}}(v_{ij}) = \int_{v_\mathrm{min}}^{v_\mathrm{max}} \int_{v_\mathrm{L}}^{v_\mathrm{H}} \frac{f_V(v_i) f_V(v_j)}{\pi} \left| \frac{\partial \Delta\phi}{\partial v_{ij}} \right| \mathrm{d}v_i \mathrm{d}v_j, \tag{6}$$

where f_V is the speed distribution, v_H and v_L are integral limits, and v_i, v_j, v_{ij}, $\Delta\phi$ has the relationship:

$$v_{ij} = \sqrt{v_i^2 + v_j^2 - 2 v_i v_j \cos(\Delta\phi)}. \tag{7}$$

The f_V in (6) is the instantaneous speed distribution that can be obtained by sampling nodes from the model. In RW or RWP there is also another widely used definition for speed distribution: the one that nodes follow when choosing

speeds at the beginning of each flight (usually uniform distribution for RW and RWP). We denote the former with f_V and the latter with g_V. They have the following relationship which can be easily derived from the results in [4]:

$$f_V(v) = \frac{\frac{1}{v} g_V(v)}{\int_{v_{\min}}^{v_{\max}} \frac{1}{v} g_V(v) \mathrm{d}v}. \tag{8}$$

2.3 Tail Behavior of Contact Time Distribution

Generally the PDF of contact time in RW can only be obtained numerically through (3). However, most implementation of RW models assume homogeneous speeds or uniform speeds, thus their the contact time distribution can be shown to have a power-law tail.

Random Walk with Homogeneous Speeds. When every node is moving at the same speed v_0, the derivation is greatly simplified. A closed form of the PDF of contact time has been derived in [18]:

$$f_{T_{\mathrm{I}}}(t_{\mathrm{I}}) = \frac{1}{4}\left(\frac{1}{t_0} + \frac{t_0}{t_{\mathrm{I}}^2}\right) \log \frac{t_0 + t_{\mathrm{I}}}{|t_0 - t_{\mathrm{I}}|} - \frac{1}{2t_{\mathrm{I}}}, \tag{9}$$

where $t_0 = r/v_0$, r is the contact range. The PDF (9) has a maximum at $t_{\mathrm{I}} = t_0$. By applying Taylor series the PDF (9) will follow a power law distribution in its tail:

$$\begin{aligned} f_{T_{\mathrm{I}}}(t_{\mathrm{I}}) &\cong \frac{1}{4}\left(\frac{1}{t_0} + \frac{t_0}{t_{\mathrm{I}}^2}\right)\left(2\frac{t_0}{t_{\mathrm{I}}} + \frac{2}{3}\left(\frac{t_0}{t_{\mathrm{I}}}\right)^3\right) - \frac{1}{2t_{\mathrm{I}}} \\ &\cong \frac{2t_0^2}{3t_{\mathrm{I}}^3} \qquad \text{when} \quad t_{\mathrm{I}} \gg t_0. \end{aligned} \tag{10}$$

Random Walk with Uniform Speeds. In most RW models nodes choose their speeds according to a uniform distribution on $[v_{\min}, v_{\max}]$ at the beginning of their flights. Therefore from (8) the instantaneous nodal speed distribution is:

$$g_V(v) = \frac{1}{v_{\max} - v_{\min}}, \tag{11}$$

$$f_V(v) = \frac{1}{v \log H}, \qquad \text{where} \quad H = \frac{v_{\max}}{v_{\min}}. \tag{12}$$

From (7) the partial derivative in (6) can be determined:

$$\Delta\phi = \cos^{-1} \frac{v_i^2 + v_j^2 - v_{ij}^2}{2v_i v_j}, \tag{13}$$

$$\frac{\partial \Delta\phi}{\partial v_{ij}} = \frac{2v_{ij}}{\sqrt{-v_i^4 - v_j^4 - v_{ij}^4 + 2v_i^2 v_j^2 + 2v_i^2 v_{ij}^2 + 2v_j^2 v_{ij}^2}}. \tag{14}$$

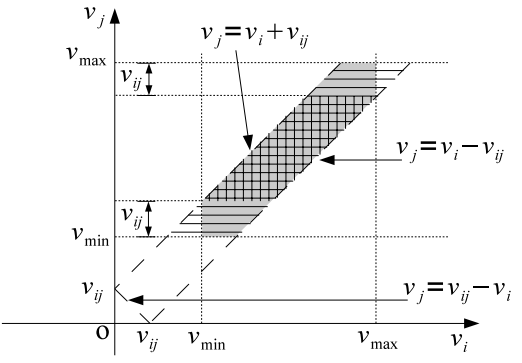

Fig. 2. The integral interval in (15) assuming $v_{ij} \leq v_{\min}$. When v_{ij} is given, v_i and v_j have to satisfy (16) so the integral interval is the gray hexagon. Alternatively, the upper and lower bound of (15) can be obtained by integration over the horizontally hatched area and vertically hatched area, respectively.

Substitute (12) and (14) into (6), the PDF of the relative speed v_{ij} is:

$$f_{V_{ij}}(v_{ij}) = \int_{v_{\min}}^{v_{\max}} \int_{v_{\mathrm{L}}}^{v_{\mathrm{H}}} \frac{2v_{ij}\mathrm{d}v_i\mathrm{d}v_j}{\pi v_i v_j \log^2 H \sqrt{-v_i^4 - v_j^4 - v_{ij}^4 + 2v_i^2 v_j^2 + 2v_i^2 v_{ij}^2 + 2v_j^2 v_{ij}^2}}. \tag{15}$$

The integral limits v_{L} and v_{H} in (15) are determined by not only $v_{\min}$ and $v_{\max}$, but also the triangle law among v_i, v_j and v_{ij}:

$$\begin{cases} v_i + v_j \geq v_{ij}, \\ v_i + v_{ij} \geq v_j, \\ v_j + v_{ij} \geq v_i. \end{cases} \tag{16}$$

Therefore the interval varies as v_{ij} varies. Since only the tail behavior of the PDF of contact time is interested, v_{ij} is assumed to be small ($v_{ij} \leq \min\{(v_{\max} - v_{\min})/2, v_{\min}\}$) and the corresponding interval is the gray hexagon in Fig. 2. To facilitate the derivation, the upper and lower bound of (15) are obtained by integration over the vertically hatched parallelogram and the horizontally hatched parallelogram in Fig. 2, respectively:

$$\begin{aligned} f_{V_{ij}}(v_{ij}) &< \int_{v_{\min}}^{v_{\max}} \int_{v_j - v_{ij}}^{v_j + v_{ij}} f_{V_i,V_j,V_{ij}}(v_i, v_j, v_{ij})\mathrm{d}v_i\mathrm{d}v_j \\ &= \frac{\log \frac{v_{\max}^2 - v_{ij}^2}{v_{\min}^2 - v_{ij}^2} - 2\log H}{2v_{ij}\log^2 H}, \\ f_{V_{ij}}(v_{ij}) &> \int_{v_{\min}+v_{ij}}^{v_{\max}-v_{ij}} \int_{v_j - v_{ij}}^{v_j + v_{ij}} f_{V_i,V_j,V_{ij}}(v_i, v_j, v_{ij})\mathrm{d}v_i\mathrm{d}v_j \end{aligned} \tag{17}$$

$$= \frac{\log \frac{v_{\max}^2 - 2v_{ij}v_{\max}}{v_{\min}^2 + 2v_{ij}v_{\min}} - 2\log \frac{v_{\max} - v_{ij}}{v_{\min} + v_{ij}}}{2v_{ij}\log^2 H}. \tag{18}$$

Applying the Taylor series:

$$f_{V_{ij}}(v_{ij}) < \frac{v_{ij}\left(\frac{1}{v_{\min}^2} - \frac{1}{v_{\max}^2}\right)}{2\log^2 H} + \mathrm{O}(v_{ij}^3), \tag{19}$$

$$f_{V_{ij}}(v_{ij}) > \frac{v_{ij}\left(\frac{1}{v_{\min}^2} - \frac{1}{v_{\max}^2}\right) - 2v_{ij}^2\left(\frac{1}{v_{\min}^3} - \frac{1}{v_{\max}^3}\right)}{2\log^2 H} + \mathrm{O}(v_{ij}^3). \tag{20}$$

Substituting (19) and (20) into (5), the corresponding upper and lower bound for the PDF of traversal speeds during *contact events* $f_{V_\mathrm{r}}(v_\mathrm{r})$ are:

$$f_{V_\mathrm{r}}(v_\mathrm{r}) < K_1 v_\mathrm{r}^2 + \mathrm{O}(v_\mathrm{r}^4), \tag{21}$$

$$f_{V_\mathrm{r}}(v_\mathrm{r}) > K_1 v_\mathrm{r}^2 - K_2 v_\mathrm{r}^3 + \mathrm{O}(v_\mathrm{r}^4), \tag{22}$$

where K_1 and K_2 are constants. As $v_\mathrm{r} \to 0$, the upper and lower bounds converge to:

$$f_{V_\mathrm{r}}(v_\mathrm{r}) \cong K_1 v_\mathrm{r}^2 + \mathrm{O}(v_\mathrm{r}^3). \tag{23}$$

Substituting (23) and (4) into (3), the asymptotic distribution of contact time t_I as $t_\mathrm{I} \to \infty$ is:

$$f_{T_\mathrm{I}}(t_\mathrm{I}) \cong \frac{K}{t_\mathrm{I}^4}, \tag{24}$$

where K is a constant.

From (24) and (10) the contact time t_I follows a power-law of t_I^{-4} with uniform speed distribution, while a power-law of t_I^{-3} with homogeneous speed. Simulation in Section 3.1 will show that the actual tail of the PDF of t_I with uniform speed distribution will first follow a power-law of t_I^{-3}, then switches to t_I^{-4}. With larger $v_{\min}$ and $v_{\max}/v_{\min}$ ratio, the transition takes place sooner.

2.4 Random Walk with Finite Flight Lengths

The analysis in previous sections is based on the assumption that nodal flight distances approach infinity such that contact events can be modeled as direct traversals. However, for most real scenarios and practical RW and RWP implementations, the flight lengths are finite. Typical RW models may have flight lengths following common distributions, like uniform, exponential, power-law, etc. Recent studies [22, 5] suggest that real world human movements can be approximated by truncated levy walks.

Regardless of how flight lengths are distributed, some traversing events will be interrupted because one or both nodes finish their current flights and change directions during the traversal. Intuitively, the longer a traversing event is, the more likely it be interrupted. When such interruption rate has reached a certain extent, the direct traversal assumption no longer holds and the contact events have to be modeled differently, e.g., as the sum of random walks.

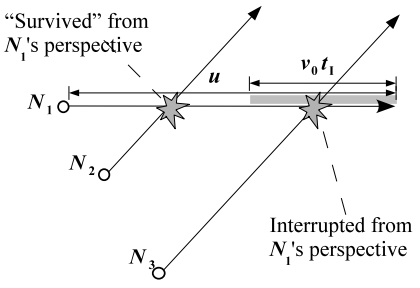

Fig. 3. Nodes N_2 and N_3 are both traversing the contact region of N_1. Both events will have the same duration t_I if not interrupted. But the traversal between N_3 and N_1 is interrupted since N_1 finishes its flight before the traversal ends.

Traversal Survival Rate. When all nodes have infinite flight lengths, assume a traversing event has duration t_I. When flight lengths are no longer infinite, we define the *survival rate* as the probability that such a traversal *not* be interrupted, which is a function of t_I, denoted with $\sigma(t_\mathrm{I})$.

At the beginning of such a traversal, both nodes are on their own flights. The traversal will "survive" only if t_I is no greater than *both* residual flight times, where by residual flight time we refer to the remaining time in the current flight. As shown in Fig. 3, N_1 is on its flight with distance u and speed v_0, while N_2 and N_3 are traversing the contact region of N_1. Both traversals have the same duration t_I if not interrupted. We further assume N_2 and N_3 have infinite flight lengths. Therefore, the traversal between N_3 and N_1 is interrupted since N_1 finishes its flight before the traversal ends, while the one between N_2 and N_1 is "survived". We denote such a survival rate when only one node has finite flight lengths with $\mu(t_\mathrm{I})$. Since nodes move independently, we have:

$$\sigma(t_\mathrm{I}) = \mu^2(t_\mathrm{I}). \tag{25}$$

Intuitively as shown in Fig. 3, all such traversals with duration t_I will be interrupted because of N_1 only if N_1 is in the gray segment at the beginning of the traversals. Assuming such traversals occur at the same frequency along that flight,[3] the survival rate along that flight with flight time $\tau = u/v_0$ is:

$$\mu(t_\mathrm{I}|\tau) = \begin{cases} \frac{\tau - t_\mathrm{I}}{\tau} & t_\mathrm{I} < \tau \\ 0 & t_\mathrm{I} \geq \tau \end{cases}. \tag{26}$$

Further, we assume that the occurrence density of traversing events of the same duration t_I is the same everywhere regardless of flight times or speeds.[4]

[3] This assumption is true for RW that has uniform node density, but not strictly true for RWP, which has higher density in the center [23]. Simulation results show that this assumption still holds sufficiently well for RWP.

[4] This assumption is strictly true only for RW with homogeneous speeds. But the results are shown to be good enough for general RW and RWP models in simulation.

We denote this density with $\eta(t_\mathrm{I})$, which is proportional to the PDF of t_I in (3) ((3) is in fact the normalized form of $\eta(t_\mathrm{I})$). Therefore the survival rate from a single node's perspective $\mu(t_\mathrm{I})$ can be derived:

$$\begin{aligned}\mu(t_\mathrm{I}) &= \frac{\int_{t_\mathrm{I}}^{\tau_\mathrm{max}} \eta(t_\mathrm{I})(\tau - t_\mathrm{I}) f_\tau(\tau)\mathrm{d}\tau}{\int_{\tau_\mathrm{min}}^{\tau_\mathrm{max}} \eta(t_\mathrm{I})\tau f_\tau(\tau)\mathrm{d}\tau} \\ &= \frac{\int_{t_\mathrm{I}}^{\tau_\mathrm{max}} (\tau - t_\mathrm{I}) f_\tau(\tau)\mathrm{d}\tau}{E(\tau)},\end{aligned} \tag{27}$$

where f_τ is the PDF of flight time. Substitute (27) into (25) the survival rate is:

$$\sigma(t_\mathrm{I}) = \mu^2(t_\mathrm{I}) = \left(\frac{\int_{t_\mathrm{I}}^{\tau_\mathrm{max}} (\tau - t_\mathrm{I}) f_\tau(\tau)\mathrm{d}\tau}{E(\tau)}\right)^2. \tag{28}$$

It is hard to directly verify (28) through simulation. Practically (28) can be verified more accurately through the duration distribution of the "survived" traversals, which is denoted with t_S:

$$f_{T_\mathrm{S}}(t_\mathrm{S}) = \frac{f_{T_\mathrm{I}}(t_\mathrm{S})\sigma(t_\mathrm{S})}{\int_0^{\tau_\mathrm{max}} f_{T_\mathrm{I}}(t_\mathrm{S})\sigma(t_\mathrm{S})\mathrm{d}t_\mathrm{S}}. \tag{29}$$

Dichotomy in the Tail. The survival rate $\sigma(t_\mathrm{I})$ calculated in (28) is a monotonically decreasing function. When the traversal duration t_I reaches a critical point t_C, the survival rate σ falls below a certain threshold γ:

$$\sigma(t_\mathrm{C}) = \gamma. \tag{30}$$

For RW with homogeneous speeds v_0, the critical point t_C has closed form when the flight length u follow some common distributions:

$$t_\mathrm{C} = \begin{cases} \frac{u_0(1-\sqrt{\gamma})}{v_0} & u \text{ fixed to } u_0, \\ \frac{2u_0}{v_0}(1 - \sqrt[4]{\gamma}) & f_U(u) = \frac{1}{2u_0},\ 0 \le u \le 2u_0, \\ -\frac{u_0}{2v_0}\log\gamma & f_U(u) = \frac{1}{u_0}e^{-\frac{u}{u_0}}. \end{cases} \tag{31}$$

The threshold γ is determined empirically. Our simulation results suggest $\gamma \le 50\%$ for most RW and RWP models.

Most of the traversals with duration $t_\mathrm{I} \ge t_\mathrm{C}$ are interrupted and their actual contact time t may follow some other distribution. Some of them may have the contact time $t < t_\mathrm{C}$. Since the PDF of t_I is fast dropping (t_I^{-3} or t_I^{-4}), the total number of events with traversal duration $t_\mathrm{I} \ge t_\mathrm{C}$ is small enough in comparison to the shorter ones. Therefore the distortion to the power-law distribution of contact times $t \le t_\mathrm{C}$ can be neglected. Thus, the tail behavior of contact times will show a dichotomy: power-law before t_C, and something else thereafter.

In [25] the authors used a finite time renewing process to obtain the upper bound of inter-contact time distribution. The same technique can also be applied

here to obtain the upper bound of the PDF of contact time t when $t > t_C$. Assume nodes are moving on a finitely bounded surface with average flight time $E[\tau]$. Consider a node N_1 at the position $X_1(t_0)$ at time t_0. After a period $t_R \gg E[\tau]$, it is reasonable to conclude that N_1's position $X_1(t_0 + T)$ is independent of $X_1(t_0)$. From the stationary nodal distribution the probability that two nodes are within the contact range of one another is p_c. Thus the probability that two nodes N_1 and N_2 kept contact with each other for time T has an upper bound:

$$P(t \geq T) \leq p_c^{T/t_R}, \tag{32}$$

which follows an exponential distribution. The parameter t_R is determined by both the boundary of the surface and the average flight time $E[\tau]$. The probability p_c is determined by $E[\tau]$ and the communication range r. Therefore, we conclude that the PDF of contact time for general RW models will exhibit a *power-law-sub-exponential dichotomy* in the tail. In fact, as simulation results shown in Section 3.2, the second half of the dichotomy can be well approximated by an exponential distribution.

Qualitatively, as average flight length $E[\tau]$ gets smaller, the power-law-sub-exponential transition takes place earlier. When the average flight length become so small (usually smaller than the contact range) that the power-law part is no longer distinguishable, the dichotomy degenerates to a single exponential tail. In this case the contact events can be modeled as the sum of consecutive random walks, and a more accurate result is obtained in [21], where the PDF of contact times follows the exponential distribution:

$$f_T(t) \cong e^{-\lambda t}, \tag{33}$$

$$\text{where } \lambda = \frac{E[v]}{r}. \tag{34}$$

$E[v]$ is the average nodal speed, and r is the contact range.

3 Validation

In this section the results in Section 2 are validated through simulation. In Section 3.1 we validate the conclusion of power-law tail assuming infinite flight lengths, and in Section 3.2 we validate the conclusion of dichotomy.

3.1 Infinite Flight Lengths without Pause

To validate the conclusion of power-law tail in Section 2.3, we implemented an RW and an RWP model. Since the assumption of infinite flight lengths is equivalent to all direct traversals not being interrupted, for each traversing event we recorded the traversing chord length s and the relative speed v_r, and calculated its traversal time t_I through (2). By doing this instead of actually implementing infinite flight lengths, the implementation is greatly simplified. In addition, it ensures that (8)

holds since nodes change their speeds between flights, therefore truly reflects the *limit of the PDF of contact time as flight lengths approach infinity.*

The RW model was on a 10×10m torus and the RWP model was on a 10×10m square. Both models have 100 nodes with communication range $r = 1$m run for 10 hours without pause. In the RW model all flights have fixed flight length $u = 10$m. In both models nodes select their speeds for each flight uniformly from $[v_{\min}, v_{\max}]$. Both models were run multiple times with different $H = v_{\max}/v_{\min}$, but with the same average speed v_{avg} derived in [4]:

$$v_{\text{avg}} = \int_{v_{\min}}^{v_{\max}} v f_V(v)\mathrm{d}v = \frac{v_{\max} - v_{\min}}{\log H}. \tag{35}$$

In our simulation $v_{\text{avg}} = 1$m/s. When $H = 1$ the models are equivalent to homogeneous speeds with speed $v_0 = 1$m/s.

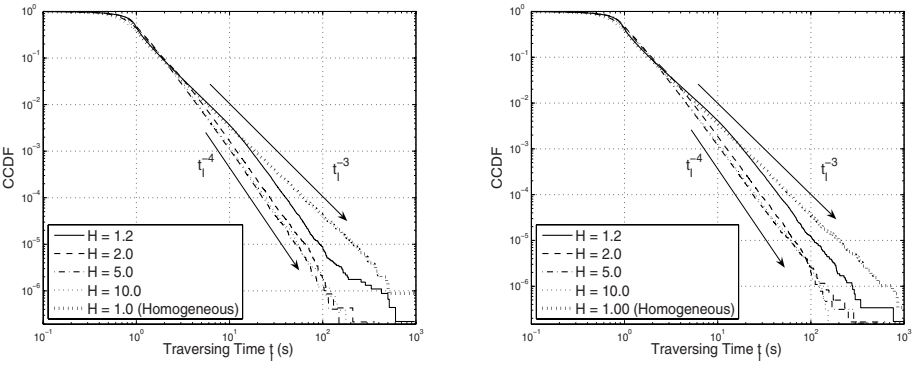

(a) (b)

Fig. 4. CCDF of t_{I} with heterogeneous speeds and without pause, with flight lengths approaching infinity. (a) Results of the RW model, (b) results of the RWP model.

The CCDFs of traversal duration t_{I} are shown in Fig. 4 on logarithmic scale. It is clearly shown that all CCDFs have power-law tail. With heterogeneous speeds the distribution functions first approach t_{I}^{-3} as with homogeneous speeds ($H = 1$), then switch to t_{I}^{-4} at some time. As H becomes larger, the distribution functions switch to t_{I}^{-4} earlier.

3.2 Finite Flight Lengths without Pause

The same models are used as in the previous section to validate the dichotomy conclusion in Section 2.4. Since the flight lengths are finite, we no longer calculate the traversal duration t_{I}, but instead directly measure the contact times t. We also diversify the random walk model by implementing different flight lengths: one RW model with uniform flight lengths on $[0, 2u]$, denoted with RWA; and

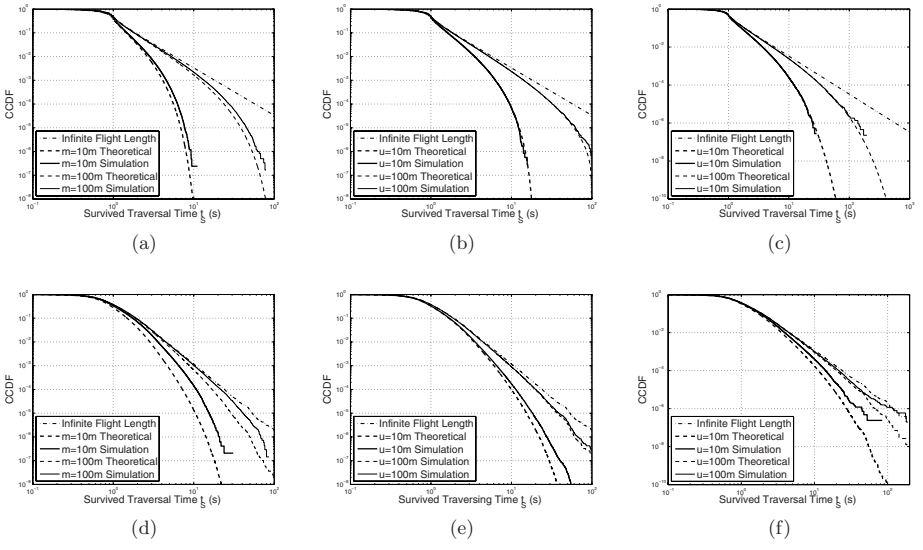

Fig. 5. CCDF of uninterrupted traversal duration t_S. Speed parameter $H = 1$ (homogeneous speeds) for (a) (b) (c) and $H = 10$ for (d) (e) (f). Mobility models: (a) (d) RWP, (b) (e) RWA, (c) (f) RWB. All with contact range $r = 1$m.

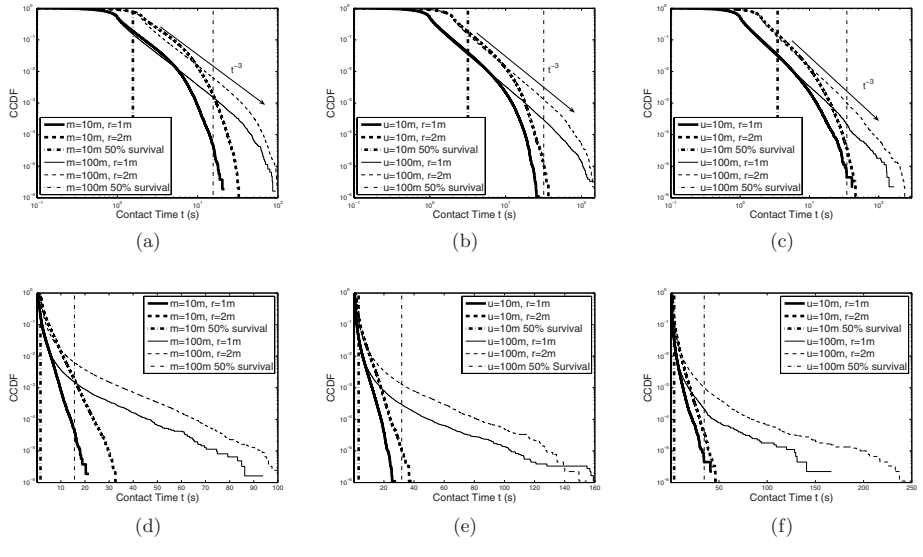

Fig. 6. CCDF of contact times for models with homogeneous speeds ($H = 1$) on logarithm plots (a) (b) (c) and semi logarithm plots (d) (e) (f). The vertical lines are the critical points t_C where the survival rate $\sigma(t_C) = 50\%$. Mobility models: (a) (d) RWP, (b) (e) RWA, (c) (f) RWB.

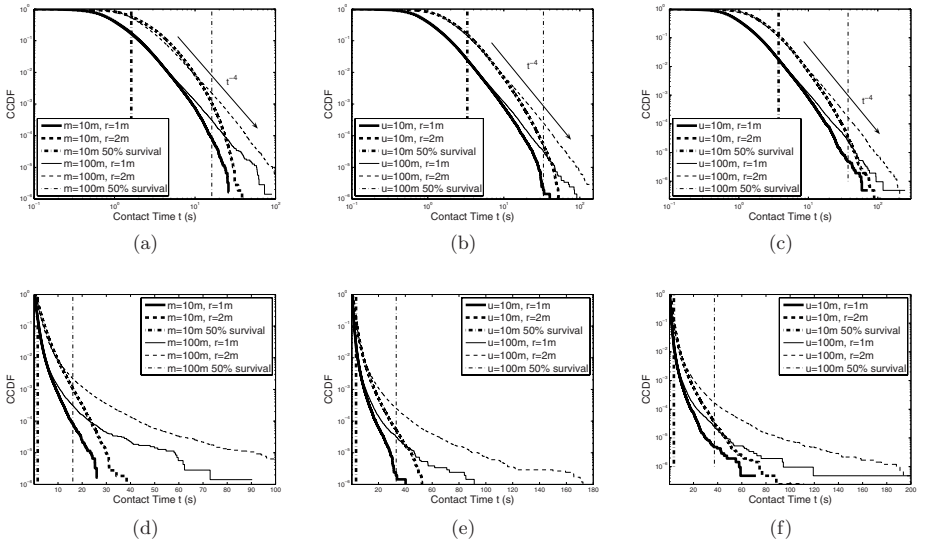

Fig. 7. CCDF of contact times for models with heterogeneous speeds ($H = 10$) on logarithm plots (a) (b) (c) and semi logarithm plots (d) (e) (f). The vertical lines are the critical points t_C where the survival rate $\sigma(t_C) = 50\%$. Mobility models: (a) (d) RWP, (b) (e) RWA, (c) (f) RWB.

one with exponential flight lengths with mean u, denoted with RWB. For the RWP model, we diversify its flight lengths by varying its area $m \times m$. In addition, the contact range r is also set to different values to compare the results.

Traversal Survival Rate. We start by validating the traversal survival rate $\sigma(t_I)$ through the uninterrupted traversal duration t_S, whose PDF is derived in (29). The CCDFs of t_S are shown on logarithmic scale in Fig. 5 together with the theoretical results. It is shown that for all RW models with homogeneous speeds, the simulation results are very close to the theoretical predictions; but for RW with heterogeneous speeds or RWP models, there are slight differences between the theoretical and simulation results. That is due to the simplifying assumptions do not strictly hold true for RWP or heterogeneous speeds as discussed in Section 2.4. However, from the results shown, (28) still holds sufficiently well to reach the conclusion of dichotomy even with RWP or heterogeneous speed.

Dichotomy in the Tail. The CCDFs of the contact time are plotted in Fig. 6 and Fig. 7 for models with different speed parameter H, contact range r and flight length u in both logarithmic scale and semi logarithmic scale. The critical points t_C where the survival rate $\sigma(t_C) = 50\%$ are also plotted as the vertical lines. From the logarithm plots the dichotomy is clearly shown in the tail of the CCDFs. When the same plots are shown on semi logarithm plots, the straight lines in the tail suggest the sub-exponential half of the dichotomy may be very close to exponential.

4 Conclusion and Future Work

In this paper we conducted a mathematical analysis of contact time distribution in random walk models, in the hope of bridging the gap between two existing approaches: the direct traversal model and the consecutive random walk model. We show that with uniform speed distribution under the direct traversal model the PDF of contact times has a power-law tail, while previous works show an exponential tail under the consecutive random walk model. We conclude that for general random walks with uniform speed distribution, the PDF of contact times has a tail that is actually between the two extremes: a power-law-sub-exponential dichotomy, which degenerates into the extremes as the flight lengths vary. This conclusion is also validated against RWP models.

Since the parameters for the sub-exponential half of the dichotomy are still not quantitatively clear, a more comprehensive analysis for that part should be done in the future. Future work should also take the pause time into consideration, since it is one of the standard components of RW and RWP models. Also, the implication of such tail behavior of contact time distribution to MANET or DTN performance is also to be studied.

References

1. Bai, F., Sadagopan, N., Helmy, A.: IMPORTANT: A Framework to Systematically Analyze the Impact of Mobility on Performance of Routing Protocols for Ad Hoc Networks. In: Proc. IEEE INFOCOM 2003, San Francisco, CA (2003)
2. Camp, T., Boleng, J., Davies, V.: A Survey of Mobility Models for Ad Hoc Network Research. Wireless Communications and Mobile Computing 2, 483–502 (2002)
3. Bai, F., Helmy, A.: Wireless Ad Hoc and Sensor Networks. Kluwer Academic Publishers, Norwell (2004)
4. Yoon, J., Liu, M., Noble, B.: Random Waypoint Considered Harmful. In: Proc. IEEE INFOCOM 2003, San Francisco, CA (2003)
5. Rhee, I., Shin, M., Hong, S., Lee, K., Chong, S.: On the Levy-walk Nature of Human Mobility. In: Proc. IEEE INFOCOM 2008, Phoenix, AZ (2008)
6. Yoon, J., Liu, M., Noble, B.: Sound Mobility Models. In: Proc. ACM MOBICOM 2003, San Diego, CA (2003)
7. Kim, M., Kotz, D., Kim, S.: Extract a Mobility Model from Real User Traces. In: Proc. IEEE INFOCOM 2006, Barcelona, Spain (2006)
8. Musolesi, M., Mascolo, C.: Designing Mobility Models Based on Social Network Theory. Mobile Computing and Communications Review 11, 59–70 (2007)
9. Zhao, M., Wang, W.: A Novel Semi-Markov Smooth Mobility Model for Mobile Ad Hoc Networks. In: Proc. IEEE GLOBECOM 2006, San Francisco, CA (2006)
10. Yoon, J., Noble, B.D., Liu, M., Kim, M.: Building Realistic Mobility Models from Coarse-Grained Traces. In: Proc. ACM MOBISYS 2006, Uppsala, Sweden (2006)
11. Hui, P., Chaintreau, A., Scott, J., Gass, R., Crowcroft, J., Diot, C.: Pocket Switched Networks and Human Mobility. In: Conference environments. Proc. ACM SIGCOMM 2005 workshop on Delay-tolerant networking, Philadelphia, PA (2005)
12. Chaintreau, A., Hui, P., Crowcroft, J., Diot, C., Gass, R., Scott, J.: Impact of Human Mobility on Opportunistic Forwarding Algorithms. IEEE Transactions on Mobile Computing 6, 606–620 (2007)

13. McDonald, A.B., Znati, T.: Link Availability Model for Wireless Ad-Hoc Networks. Technical Report, TR 99-07. University of Pittsburgh, Pittsburgh, PA (1999)
14. Gruber, I., Li, H.: Link Expiration Times in Mobile Ad Hoc Networks. In: Proc. IEEE LCN 2002, Los Alamitos, CA (2002)
15. Sadagopan, N., Bai, F., Krishnamachari, B., Helmy, A.: PATHS: Analysis of Path Duration Statistics and Their Impact on Reactive MANET Routing Protocols. In: Proc. IEEE MOBIHOC 2003, Annapolis, MD (2003)
16. Samar, P., Wicker, S.B.: On the Behavior of Communication Links of a Node in a Multi-Hop Mobile Environment. In: Proc. IEEE MOBIHOC 2004, Roppongi, Japan (2004)
17. Samar, P., Wicker, S.B.: Link Dynamics and Protocol Design in a Multihop Mobile Environment. IEEE Transactions on Mobile Computing 5, 1156–1172 (2006)
18. Tsao, C.L., Wu, Y.T., Liao, W., Kuo, J.C.: Link Duration of the Random Way Point Model in Mobile Ad Hoc Networks. In: Proc. IEEE WCNC 2006, Las Vegas, NV (2006)
19. Triviño-Cabrera, A., García-de-la-Nava, J., Casilari, E., González-Cañete, F.J.: An Analytical Model to Estimate Path Duration in MANETs. In: Proc. ACM MSWiM 2006, Torremolinos, Málaga, Spain (2006)
20. Wu, X., Sadjadpour, H.R., Garcia-Luna-Aceves, J.: From Link Dynamics to Path Lifetime and Packet-Length Optimization in MANETs. Wireless Networks 15(5), 637–650 (2007)
21. Wang, W., Zhao, M.: Joint Effects of Radio Channels and Node Mobility on Link Dynamics in Wireless Networks. In: Proc. IEEE INFOCOM 2008, Phoenix, AZ (2008)
22. González, M.C., Hidalgo, C.A., Barabási, A.L.: Understanding Individual Human Mobility Patterns. Nature 453, 779–782 (2008)
23. Bettstetter, C., Resta, G., Santi, P.: The Node Distribution of the Random Waypoint Mobility Model for Wireless Ad Hoc Networks. Mobile Computing and Communications Review 2, 257–269 (2003)
24. Bettstetter, C., Hartenstein, H., Pérez-Costa, P.: Stochastic Properties of the Random Waypoint Mobility Model. Wireless Networks 10, 555–567 (2004)
25. Cai, H., Eun, D.Y.: Crossing Over the Bounded Domain: From Exponential to Power-Law Inter-Meeting Time in MANET. In: Proc. ACM MOBICOM 2007, Montréal, Canada (2007)